Exciton Fine Structure in Single CdSe Nanorods

N. Le Thomas, E. Herz, O. Schöps, and U. Woggon*
Fachbereich Physik, Universität Dortmund, Otto-Hahn-Strasse 4, 44227 Dortmund, Germany

M. V. Artemyev
Institute for Physico-Chemical Problems of Belorussian State University, Minsk 220080, Belarus
(Received 13 July 2004; published 5 January 2005)

We study the optical properties of excitons in one-dimensional (1D) nanostructures at low temperatures. In single CdSe/ZnS core-shell nanorods we observe a fine structure splitting and explain it by exchange interaction. Two peaks are observed with different degrees of linear polarization of DLP < 0.85 and DLP > 0.95. For small nanorod radii $R \leq a_B/2$, an increase in the photoluminescence decay time is found when the temperature increases from 10 to 80 K. The observations are explained by a radius-dependent change in the symmetry of the 1D-exciton ground state which transforms from a dark state into bright states below a critical radius of $R_{crit} \approx 3.7$ nm.

DOI: 10.1103/PhysRevLett.94.016803 PACS numbers: 73.22.–f, 42.60.Da, 42.70.–a, 78.67.–n

Quantum-confined nanoparticles are being increasingly investigated due to the superior efficiency and tunability of their emission spectra from the ultraviolet to the near infrared. Such nanoparticles include quantum dots, nanorods, or quantum wires. Recently, CdSe nanorods (NRs) have been studied due to their excellent optical properties, which are, e.g., emission of highly polarized light, potential as a low-threshold material in nanocrystal-based lasers, and large permanent dipole moment [1–7]. The quantum nature of an emitting state in a 1D nanostructure is also of fundamental interest. Since the size-dependent 1D-exciton fine structure defines the eigenstate symmetry, the oscillator strength and the level structure of the exciton ground state, a detailed understanding of this size dependence is crucial for defining threshold conditions in NR lasers, fluorescent labeling, quantum optics, and in polarization-sensitive marking and detecting devices. To control the quantum efficiency, the degree of polarization or the relaxation dynamics as a function of nanocrystal shape *and* size, the exchange interaction has to be analyzed and understood in detail. While intensive experimental and theoretical work has been performed to describe the excitonic exchange interaction in spherical nanocrystals (NCs) (see, e.g., [8–10]), the exchange interaction in quantum-confined NRs and its consequences for the optical spectra have not been measured up to now.

In this work we present low-temperature, polarization-sensitive photoluminescence spectroscopy of single CdSe(ZnS) core-shell nanorods. The single NR line shape has been determined, and a fine structure is found, which we assign to exchange splitting of a 1D exciton confined in a cylindrical CdSe nanorod. The measured degree of polarization, the radius-dependent change in ground state symmetry, and the observed increase in photoluminescence decay time with increasing temperature are all explained by the 1D-exciton confinement and exchange interaction.

We investigate CdSe/ZnS core-shell NRs at cryogenic temperatures which were prepared according to Ref. [11] and dispersed in a thin film of poly(butyl methacrylate-comethyl methacrylate). The NRs were excited by the 488 nm line of an argon-ion laser at an intensity of ~ 10 W/cm^2 for measuring the single rod spectra, and by a 150 fs pulse of a frequency-doubled Ti:Sa laser for studying the emission dynamics. In order to analyze the polarization properties in microphotoluminescence (μ-PL), a birefringent calcite plate was used at the spectrometer entrance to split the μ-PL signal into two perpendicularly polarized beams $I_{\parallel}$ and $I_{\perp}$. The polarization is studied using a $\lambda/2$ plate in the detection beam path of the μ-PL setup.

Figure 1 shows a single NR emission spectrum recorded in 1 s intervals at $T = 15$ K. The corresponding ensemble

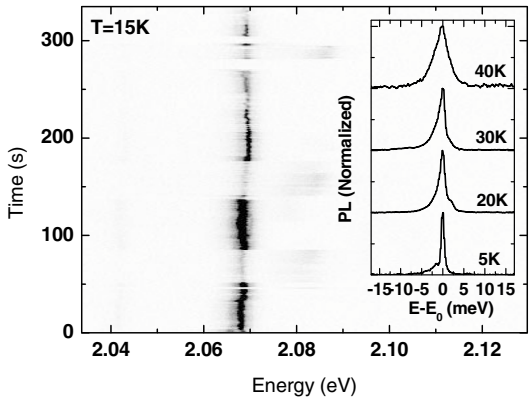

FIG. 1. Spectrally resolved intensity versus time (linear gray-scale-coded plot) of a single CdSe NR (radius $R \sim 2.5$ nm, length $L \sim 25$ nm) at $T = 15$ K. Each spectrum is taken using an imaging spectrometer with a charge coupled device camera and acquisition time of 1 s. The total collected intensity is ~ 300 counts/s. The inset shows NR spectra at different temperatures.

emission has its spectral maximum at 2.03 eV with an inhomogeneous broadening of ~80 meV. The average NR radius of $R = 2.5 \pm 0.3$ nm and length of $L = 25 \pm 0.3$ nm are deduced from transmission electron microscopy data in agreement with recent spectroscopic data from Ref. [12]. As can be seen, the spectral wandering is small and stays within an interval of 3 meV. The inset shows single NR spectra at different temperatures showing a non-Lorentzian line shape. When the temperature is increased, the contribution from an acoustic phonon sideband increases relative to the sharp (resolution-limited) zero-phonon line (ZPL), very similar to that observed for II-VI quantum dots in Ref. [13].

Figure 2 shows the line shape of low-temperature single NR emission spectra in detail. Among the 30 individually measured NRs, whose energy distribution is shown in the inset of Fig. 2, two different groups of single NR spectra are observed (labeled S* and S) and characterized by a strong line shape difference. At the lowest temperature the S*-type spectrum is composed of a ZPL and an acoustic phonon sideband only, whereas the S-type main peak, observed for about 30% of NRs, splits into two peaks with different polarization properties. The S*-type spectrum could be attributed to a charged exciton, where all fine structure resulting from the electron-hole exchange interaction are expected to vanish due to the excess carrier present. For some NRs the observed spectral jumps between S*-type and S-type spectra are consistent with an excess charge transfer into the surroundings.

We focus here on the single NR spectrum of S type that shows a fine structure for $T < 15$ K. In this case the time-integrated μ-PL spectrum is composed of a main peak labeled S_0, a second peak S_1 and a weak peak S_{LO} redshifted by 28.4 meV with respect to S_0. A spectral jitter correlation technique (see [14]) gives us clear evidence that they stem from the same NR. The spectral spacing between S_1 and S_{LO} is 26.5 meV. As this energy corresponds to the LO-phonon energy in bulk CdSe material, the small peak S_{LO} is attributed to the first LO-phonon replica of S_1. For the measured NRs we observe splittings, $\Delta E = S_0 - S_1$, of between 1.4 and 2.0 meV for S_0 emission energies between 2.070 and 2.107 eV.

The polarization degree of the NR emission is analyzed in Fig. 3. The linear polarization ratio δ of the emission spectrum, defined as $\delta = (I_{\parallel} - I_{\perp})/(I_{\parallel} + I_{\perp})$, is recorded during the temporal scan of the single NR emission spectrum for simultaneous measurement of $I_{\parallel}$ and $I_{\perp}$. Plotting δ vs the polarization rotation angle θ, a very high degree of linear polarization (DLP), higher than 0.95, is revealed for the S_0 state while for the S_1 line (down triangles) the DLP has a smaller value of 0.85 as can be seen in the insets of Fig. 3. This unexpectedly high DLP value observed for S_0 is even larger than that reported for pure electronic confinement in a quantum wire. In that case a value of only DLP = 0.60 was reported for the electron-hole pair ground state transition [15]. Even when taking into account the dielectric confinement, another source of DLP enhancement as discussed in [16,17], the estimated DLP values are still lower than our experimental results. At room temperature, a DLP of 0.87 is reported [1] and also found for the NRs studied in this work [18]. At low temperature, however, S_0 almost disappears from the $I_{\perp}$ spectrum, whereas S_1 with less DLP is still visible for $\theta = 10°$ (top inset). The presence of the feature S_1 is thus not only revealed by the line shape and the LO-phonon replica spacing, but also by the DLP difference between S_0 and S_1.

To obtain data for single NRs with larger radii, μ-PL studies have been carried out with NR samples of larger average radius, e.g, $R \sim 4$ nm. However, no spectrally

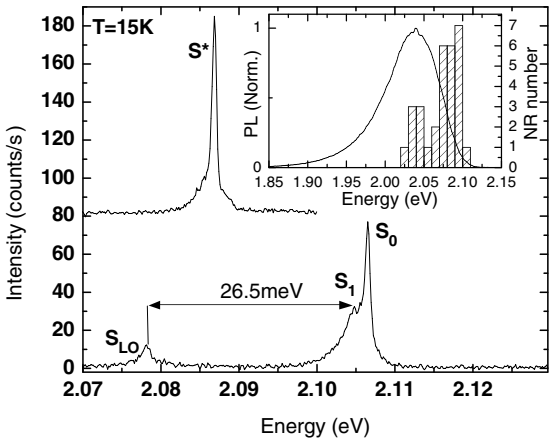

FIG. 2. Two time-integrated spectra of a single CdSe NRs recorded within a 22 s detection period at $T = 15$ K. The origin of the spectrum labeled S* has been shifted by 80 counts/s. The inset compare the energy distribution of the 30 measured single NRs with the ensemble photoluminescence.

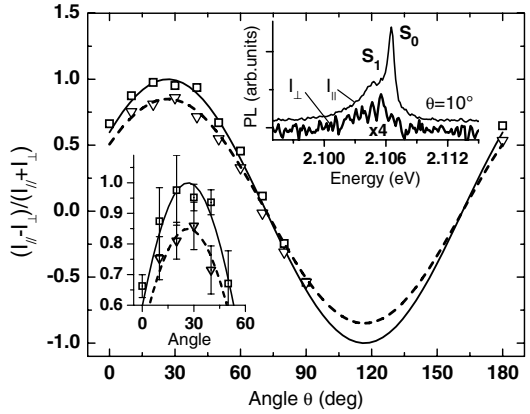

FIG. 3. Intensity ratio $\delta = (I_{\parallel} - I_{\perp})/(I_{\parallel} + I_{\perp})$ versus the polarization rotation angle θ plotted for S_0 (squares) and S_1 (down triangles). The upper inset shows the spectra for $I_{\parallel}$ and $I_{\perp}$ at $\theta = 10°$, whereas the lower inset is a zoom highlighting the DLP difference between S_0 and S_1. The difference in polarization of the S_1 peak excludes its origin from a discrete acoustic phonon mode.

sharp, single NR spectra were observed for larger R, that were photostable during more than 2 s, indicating different optical properties of small and big NRs. This hypothesis is supported by the emission dynamics of NR ensembles as we discuss next in Fig. 4. This figure shows the NR dynamics for different temperatures in comparison with spherical NCs with average radius $R \sim 3$ nm. The NC data in Fig. 4(a) can be fitted well by the standard model of thermally activated population of the bright ± 1 state from the dark ± 2 state (see the inset diagram and, e.g., [19]) which gives here for $R \sim 3$ nm NCs the radiative decay times $\tau_{\text{bright}} = 15$ ns and $\tau_{\text{dark}} = 142$ ns, respectively, an exchange splitting energy of $\Delta E = 1.4$ meV and a transfer time between these two states (requiring a spin flip) of $1/\gamma_0 = 1.4$ ns. The NC data, given here as a reference, reproduce well the known behavior of a decreasing PL-decay time as the temperature is increased due to thermally activated bright ± 1 state filling (see the scheme in the inset). In Fig. 4(b), the dots' and rods' PL-decay curves are compared for a fixed elevated temperature of 80 K. The PL decay within the first 2 orders of magnitude is the fastest for the $R \sim 4$ nm rods ($\tau \approx 5.6$ ns; see [20]) followed by the $R \sim 3$ nm dots ($\tau \approx 11.4$ ns) and the $R \sim 2.5$ nm rods ($\tau \approx 23.5$ ns). The most striking feature, however, is shown in Fig. 4(c) for small NRs with $R \sim 2.5$ nm: the decay time becomes *slower* with increasing temperature, while the opposite is observed for the larger NRs with $R \sim 4$ nm [Fig. 4(d)] whose PL dynamics are more similar to the NC dynamics. The small NR PL decay is the slowest at 80 K while it is the fastest at 5 K ($\tau \approx 3.6$ ns).

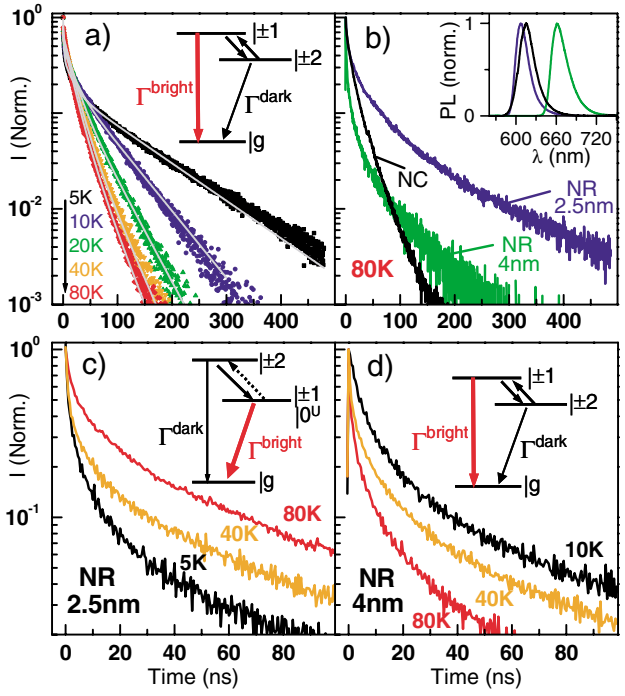

FIG. 4 (color). Ensemble photoluminescence decay at different temperatures measured by single-photon counting for different nanocrystal sizes and shapes [the PL ensemble spectra are shown in the inset of (b)]. (a) Spherical nanocrystals with $R = 3$ nm, (c) nanorods with $R = 2.5$ nm and $L = 25$ nm, and (d) nanorods with $R = 4$ nm and $L = 35$ nm. In (b) the decay is compared for a fixed temperature of 80 K.

In the following we propose an explanation of the observed spectral features and dynamics which is based on the 1D-exciton exchange interaction. In order to calculate the NR electronic levels and the effect of the exchange interaction on the lowest-energy 1D electron-hole pair states, we take advantage of the cylindrical symmetry of the system and follow the formalism developed in [15]. The hole ground state is the even state $S_{1/2}$. This state has a strong light hole character as far as optical properties are concerned. The next hole state with S symmetry, $S_{3/2}$, has a predominantly heavy hole character. In cylindrical symmetry the quantum confinement (QC) lifts the degeneracy between the $S_{3/2}$ and $S_{1/2}$ states. The contribution to the $S_{3/2}$-$S_{1/2}$ splitting from the crystal field (CF), 25 meV in bulk CdSe, is treated as a perturbation to the Luttinger Hamiltonian [9]. The electron-hole pair energy is obtained by a variational calculation following [21]. Including Coulomb interaction gives us both the information about the electron-hole pair energy and the spatial overlap between electron and hole (see the inset of Fig. 5). After deriving these 1D-exciton parameters, the electron-hole exchange interaction is calculated following the theory of invariants of Ref. [9]. The fourfold degenerate "light hole" exciton ground state $s_e S_{1/2}$ is then split into a twofold degenerate state with total angular momentum projection along the rod axis ± 1, and two other states with total

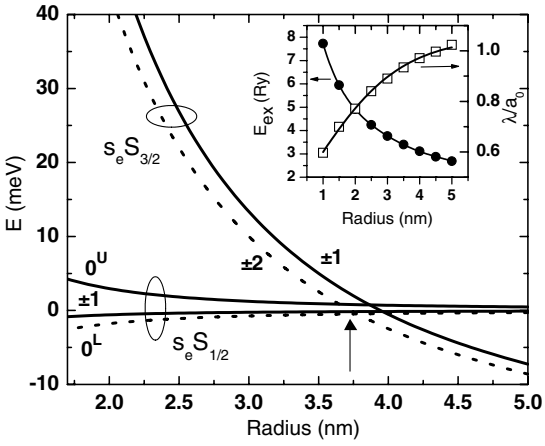

FIG. 5. Fine structure splitting of the 1D exciton. Optically dark (bright) states are plotted by dotted (solid) curves. The critical radius R_{crit} for the symmetry crossing between the ± 2 state and the 0 state is indicated by an arrow. The inset shows the 1D-exciton ground state energy (Ry ~ 15 meV) and the variational parameter λ, representing the exciton spatial extension along the NR axis, as defined in [21], versus the NR radius (excitonic Bohr radius $a_0 \sim 5.6$ nm).

angular momenta projection 0 along the rod axis labeled 0^U and 0^L (U and L denote upper and lower, respectively). The "heavy hole" exciton $s_e S_{3/2}$ splits into the optically active state with ± 1 and the optically forbidden state ± 2 commonly called a "dark" state.

In Fig. 5 the calculated energies of the $s_e S_{1/2}$ and $s_e S_{3/2}$ states are plotted versus the NR radius R relative to the $s_e S_{1/2}$ state with no exchange interaction. The most important result is a change in ground state symmetry at a radius R_{crit}, the solution of $[E_{\mathrm{QC}}^{S_{3/2}}(R) - E_{\mathrm{QC}}^{S_{1/2}}(R)] - [E_{\mathrm{ex}}^{S_{3/2}}(R) - E_{\mathrm{ex}}^{S_{1/2}}(R)] - \Delta(R) = 0$, where $E_{\mathrm{QC}}^{S_{3/2}}$ and $E_{\mathrm{QC}}^{S_{1/2}}$ are the $S_{3/2}$ and $S_{1/2}$ hole states' confinement energy, respectively, $E_{\mathrm{ex}}^{S_{3/2}}$ and $E_{\mathrm{ex}}^{S_{1/2}}$ are the exciton energies associated with the same states, and $\Delta$is the first order energy shift corresponding to the CF perturbation. Below $R_{\mathrm{crit}} \approx 3.7$ nm the dark state ± 2 is no longer the NR ground state, in contrast to spherical NCs, due to the interplay between the electronic confinement and the hexagonal crystal symmetry. While for large radius the QC is negligible and $s_e S_{3/2}$ becomes the ground state due to the CF splitting, the opposite holds for small radii and now $s_e S_{1/2}$ is the ground state. Taking into account the exchange interaction, the ground state is the 0^L state for NR radii below R_{crit} which has zero oscillator strength [9]. The small energy differences between the 0^L, ± 1, and 0^U states allow a thermal population of all three states at 15 K. As a result the lines S_1 and S_0 in Fig. 2 are attributed to the ± 1 and 0^U states. The 0^U state, whose angular momentum projection is 0, emits strictly linearly polarized photons in full agreement with the experimental data of Fig. 3. In addition, the DLP of the S_1 line is smaller because of the change in symmetry. However, it is not opposite to the S_0 DLP as expected for a circularly polarized state since the S_1 line still overlaps with the S_0 acoustic phonon sideband.

The calculated symmetry change around a critical radius R_{crit} is especially relevant for the understanding of the PL dynamics. It predicts a strong radius dependence of the PL decay time and its temperature dependence. For NR radii R below and above the bright (± 1, 0^U)-dark (± 2) state crossing in Fig. 5, the optical transition probabilities drastically change. For $R > R_{\mathrm{crit}}$ and low temperatures, a slow decay due to the dark state is expected, similar to spherical NCs shown in Fig. 4(a), which becomes faster when the temperature increases. This qualitative behavior is observed for large NRs in Fig. 4(d). For NRs of $R < R_{\mathrm{crit}}$, however, a PL-decay time acceleration is not expected because the bright states ± 1 and 0^U are energetically below the dark ± 2 state. The slowing down of the PL decay with rising temperature, observed in Fig. 4(c), is a new and interesting phenomenon which might stimulate further experimental and theoretical work. It could be explained, for example, by the model proposed in Ref. [22] which says that the exciton intrinsic radiative lifetime, τ_r, of a defect-free quantum wire is expected to rise according to $\sqrt{T}$. In the bigger nanorods this effect would be hidden by the thermal filling of the bright state. By fitting the curves in Fig. 4(c), and additional ones at 10 and 20 K [20], we found that the average decay time of τ grows as $1.2\sqrt{T}$ ns $\mathrm{K}^{-1/2}$.

In conclusion, we have studied the emission line shape and polarization of a 1D exciton in single CdSe/ZnS nanorods at low temperature and explained them by taking into account the electron-hole exchange interaction. The high degree of linear polarization (DLP > 0.95) and size or shape dependent PL decay times emphasize the important role of the exchange interaction for the understanding of optical NR properties.

Financial support by the DFG (Graduiertenkolleg GRK 726, Wo477/18), by the EU Project HPRN-CT-2002-00298, by the German-American Fulbright Commission, and by INTAS 01/2100 is gratefully acknowledged. We thank W. Langbein for discussions and experimental assistance.

*Electronic address: ulrike.woggon@uni-dortmund.de

[1] J. Hu *et al.*, Science **292**, 2060 (2001).
[2] X. Chen *et al.*, Phys. Rev. B **64**, 245304 (2001).
[3] J. Li and L. W. Wang, Nano Lett. **3**, 101 (2003).
[4] M. Califano *et al.*, Nano Lett. **3**, 1197 (2003).
[5] R. Krishnan *et al.*, Phys. Rev. Lett. **92**, 216803 (2004).
[6] L. Li and A. P. Alivisatos, Phys. Rev. Lett. **90**, 097402 (2003).
[7] M. Kazes *et al.*, Adv. Mater. **14**, 317 (2002).
[8] M. Nirmal *et al.*, Phys. Rev. Lett. **75**, 3728 (1995).
[9] Al. L. Efros *et al.*, Phys. Rev. B **54**, 4843 (1996).
[10] A. Franceschetti *et al.*, Phys. Rev. B **60**, 1819 (1999).
[11] T. Mokari and U. Banin, Chem. Mater. **15**, 3955 (2003).
[12] D. Katz *et al.*, Phys. Rev. Lett. **89**, 086801 (2002).
[13] U. Woggon *et al.*, Phys. Rev. B **54**, 1506 (1996); K. Takemoto *et al.*, Solid State Commun. **114**, 521 (2000); L. Besombes *et al.*, Phys. Rev. B **63**, 155307 (2001); P. Palinginis *et al.*, Phys. Rev. B **67**, 201307(R) (2003).
[14] B. Patton *et al.*, Phys. Rev. B **68**, 125316 (2003).
[15] P. C. Sercel and K. J. Vahala, Phys. Rev. B **44**, 5681 (1991).
[16] J. Wang, M. S. Gudiksen, X. Duan, Y. Cui, and C. M. Lieber, Science **293**, 1455 (2001).
[17] A. Shabaev and Al. L. Efros, Nano Lett. **4**, 1821 (2004).
[18] U. Woggon *et al.*, Appl. Phys. B **77**, 469 (2003).
[19] M.G. Bawendi *et al.*, J. Chem. Phys. **96**, 946 (1992); M. Nirmal *et al.*, Phys. Rev. Lett. **75**, 3728 (1995); X. Fan *et al.*, Phys. Rev. B **64**, 115310 (2001); O. Labeau *et al.*, Phys. Rev. Lett. **90**, 257404 (2003); S. A. Crooker *et al.*, Appl. Phys. Lett. **82**, 2793 (2003).
[20] The NRs's decay time is an averaged τ derived from a stretched exponential taking into account a distribution in lifetimes (details will be published elsewhere).
[21] H. Ham and H. N. Spector, Phys. Rev. B **62**, 13 599 (2000).
[22] D. S. Citrin, Phys. Rev. Lett. **69**, 3393 (1992).